University of Freiburg Preprint THEP 18/93

Fluctuation effects on wave propagation in a reaction–diffusion process

Heinz–Peter Breuer, Wolfgang Huber and Francesco Petruccione
Albert-Ludwigs-Universität, Fakultät für Physik,
Hermann-Herder-Straße 3, D–79104 Freiburg im Breisgau,
Federal Republic of Germany
August 24, 1993

Abstract

The reaction–diffusion process corresponding to the Fisher–Kolmogorov equation is studied by means of a discrete multivariate master equation. For travelling wave fronts the stability criterion necessary for the applicability of a system–size expansion is shown to be violated due to the existence of a zero mode of the first variational equation. This zero mode is connected to the translational invariance of the system. Performing stochastic simulations of the master equation in a wide range of parameters it is demonstrated that for finite size of the system (up to about 10^7 particles in the frontal region) a rather large fluctuation effect on the wave propagation speed results: In general, the asymptotic wave speed lies below the stable, minimal speed which is given by a theorem of Kolmogorov for the macroscopic equation. The wave front position exhibits a diffusion–type behaviour associated with translative fluctuations along the propagation direction.

1 Introduction

The Fisher–Kolmogorov equation represents a simple non–linear reaction–diffusion equation for a space and time dependent concentration $c(x,t)$. Its relevance stems from the fact that it admits stable travelling wave solutions which describe the spread of the substance described by the concentration $c(x,t)$. For example, it has been used to describe the wave of advance of advantageous genes [1] or the spread of neolithic farming [2]. Moreover, it is studied as a prototype to understand the qualitative behaviour of more complicated dynamics [3, 4]. Microscopic Boltzmann equation and lattice gas simulations have been reported in [5] and [6].

Mathematically, the Fisher–Kolmogorov equation is a deterministic partial differential equation. However, in most applications the variable $c(x,t)$ is defined

as the number of discrete particles, e.g. individuals or molecules, in a given volume element of space. It is this discrete nature of the dynamical variables which necessarily leads to internal fluctuations in the system and which makes a stochastic description indispensable. Within such a stochastic description $c(x,t)$ appears as the expectation value of the number of particles per volume element.

Thus, it is important to investigate the influence of internal fluctuations upon the dynamics described by the Fisher–Kolmogorov equation. This will be done in the present paper by formulating a multivariate master equation which models the diffusive part as a collective random walk process and the reactive part by means of a chemical birth–and–death process. The resulting master equation describes the reaction–diffusion process on a mesoscopic level including internal fluctuations induced by the discrete particle representation. Employing a stochastic simulation technique we investigate this multivariate stochastic process for a wide range of parameters. In particular, we study the influence of fluctuations upon the wave speed and wave front position.

Usually one argues that fluctuations are small and, therefore, it suffices to investigate the dynamics of the averages. However, this is true only if fluctuations are damped or, in other words, if the macroscopic dynamics is asymptotically stable. Under this condition the Ω–expansion provides a unique decomposition of the stochastic process into a macroscopic part which is governed by a deterministic differential equation and a small fluctuating part which obeys a linear Fokker–Planck equation describing small Gaussian fluctuations around the macroscopic dynamics. Thus, under the condition of asymptotic stability a unique macroscopic equation is extracted by means of the Ω–expansion and the influence of the noise upon the macroscopic dynamics can be completely neglected.

However, as is well-known the situation changes drastically if the macroscopic dynamics becomes unstable. This is the case, for example, if by varying some control parameter, hyperbolic fixed points emerge from bifurcations of the deterministic macroscopic equation [7, 8, 9]. The master equation investigated in this paper shows a different type of behaviour. Performing the Ω–expansion it will be shown that the condition of asymptotic stability is violated for travelling wave solutions. To be more precise, the translational invariance of the system leads to the existence of perturbations which stay constant in time rather than tending to zero. As a result the position of the wave front exhibits a diffusion–type behaviour with a strong influence upon the speed of the travelling wave. These facts are demonstrated by means of stochastic simulations of the full master equation.

The paper is organized as follows. Having briefly reviewed the basic properties of the Fisher–Kolmogorov equation in section 2 we construct in section 3 the multivariate master equation governing the stochastic process of the particle numbers. We perform its Ω–expansion and show that the condition of asymptotic stability is violated due to the existence of translative perturbations. In section IV we explain the stochastic simulation technique which is then used in order to simulate the multivariate stochastic process defined by the master equation.

The results of the simulations are discussed in view of the results of section 3. In particular, we investigate the speed of the travelling waves and the influence of translative fluctuations. In section 5 we summarize the results and draw some conclusions.

2 The Fisher–Kolmogorov equation

The rate equation that corresponds in the continuum limit to the reaction–diffusion process we will consider in the following is

$$\frac{\partial c}{\partial t} = D\frac{\partial^2 c}{\partial x^2} + Ac - Bc^2 \quad . \tag{1}$$

It is often called the *Fisher–Kolmogorov equation* [1, 10]. $c \equiv c(x,t)$ is a real-valued function of the one-dimensional space-variable x and of the time t. In applications, c is usually a concentration, so we are only interested in positive solutions. D, A and B are positive parameters which are also constant in space and time for the present discussion. As far as applications to reaction–diffusion processes are concerned the above Fisher–Kolmogorov equation describes the behaviour of the concentration $c(x,t)$ of molecules of type X which diffuse in space with diffusion constant D and react according to the scheme

$$Y \; + \; X \; \rightleftharpoons 2\,X \quad , \tag{2}$$

where A and B denote the corresponding reaction rate coefficients. The concentration of the molecules of type Y is assumed to be constant, i. e. the Y–molecules serve as a particle reservoir.

By appropriately scaling space and time and measuring c in units of the typical concentration A/B, one can reduce the number of parameters to one. If one replaces

$$x \mapsto \frac{B}{A}\,x \;, \qquad t \mapsto A\,t \;, \qquad c \mapsto \frac{A}{B}\,c \;,$$

and introduces the new dimensionless paramter

$$\gamma := \frac{DA}{B^2} \quad ,$$

equation (1) becomes

$$\frac{\partial c}{\partial t} = \gamma\frac{\partial^2 c}{\partial x^2} + c - c^2 \quad . \tag{3}$$

Equation (3) has two stationary states. One of them, $c \equiv 0$ is unstable, while the other one, $c \equiv 1$, is stable. Furthermore, eqn. (3) admits travelling wave

solutions. In a frame of reference that is moving with the constant speed v along the x–axis, eqn. (3) becomes

$$\frac{\partial \phi}{\partial t} = \gamma \frac{\partial^2 \phi}{\partial z^2} + v \frac{\partial \phi}{\partial z} + \phi - \phi^2 \quad , \tag{4}$$

where $c(x,t) = \phi(x - vt, t)$ and $z = x - vt$. A travelling wave with speed v is given by the stationary solution of eqn. (4), i. e.

$$c(x,t) = \phi(x - vt) \quad . \tag{5}$$

These travelling wave solutions connect the unstable to the stable state,

$$\lim_{x \to -\infty} c(x,t) = 1 \qquad \text{and} \qquad \lim_{x \to +\infty} c(x,t) = 0 \quad , \tag{6}$$

where we have chosen to let the front propagate from the left to the right. An essential feature of the Fisher–Kolmogorov equation is the existence of travelling wave solutions for any wave speed $v \geq v_{min} = 2\sqrt{\gamma}$ [1].

A large class of initial conditions evolves to the solution $c(x,t)$ propagating with minimum speed $v_{min} = 2\sqrt{\gamma}$. This class contains those initial conditions $c(x,0)$ that satisfy the following conditions [3, 10]:

- $c(x,0)$ non–negative and continuous everywhere,
- $c(x,0) = 1$ if $x \leq x_1$,
- $c(x,0) = 0$ if $x \geq x_2$ or $c(x,0) \propto \exp(-ax)$ as $x \to \infty$,

where $x_1 < x_2$ and $a \geq 1/\sqrt{\gamma}$. Thus the asymptotic wave speed depends sensitively on the behaviour of the initial condition $c(x,0)$ as $x \to \infty$. On the other hand side, if the initial condition is such that $c(x,0) = 0$ for $x \geq x_2$, then the ultimate wave does not depend on the detailed form of $c(x,0)$. Any practical model deals, of course, with a finite domain, and the quantity whose concentration is described by $c(x,t)$ eventually consists of discrete particles – in this sense we have always an initial condition of type: $c(x,0) = 0$ if $x \geq x_2$.

Looking at the stability of travelling wave solutions, we have just seen that they are unstable to perturbations that are nonzero for large x. However they are stable to finite domain perturbations [3]. This question becomes important in section 3 and will be addressed there in more detail.

In order to be able to speak about the front position, we introduce as a pragmatical measure for the front position at time t

$$c_{tot}(t) = \int_{x_0}^{+\infty} c(x,t) dx \quad , \tag{7}$$

where x_0 is a point far enough left of the initial front, and $c_{tot}(t)$ is the total amount of substance at time t. This allows an alternative definition of the wave propagation speed,

$$v_R = \frac{dc_{tot}(t)}{dt} = \frac{d}{dt}\int_{x_0}^{+\infty} c(x,t)dx = \int_{x_0}^{+\infty}\left(\frac{\partial^2}{\partial x^2}c + c - c^2\right)dx = \int_{x_0}^{+\infty}\left(c - c^2\right)dx \quad . \tag{8}$$

For travelling wave solutions, this is equivalent to the former definition of the wave speed eqn.(5). Moreover, it is an obvious generalization of the wave speed to solutions which are not stationary in any comoving frame.

The analytical form of travelling wave solutions is in general not known. There is one known analytical solution for $v = 5\sqrt{\gamma/6}$,

$$c(x,t) = \frac{1}{\left[1 + \exp\left(z/\sqrt{6\gamma}\right)\right]^2} \quad , \tag{9}$$

which is however not stable [3]. In the limit where the Fisher–Kolmogorov equation is a good deterministic approximation of the stochastic process (which will be discussed in more detail below), eqn. (9) is useful for getting an idea of what the wave front for a given parameter γ should look like.

3 The Master Equation

The Fisher–Kolmogorov equation introduced in section 2 constitutes a purely macroscopic, deterministic description of the reaction–diffusion process. However, in general the concentration $c(x,t)$ describes some average value of a *discrete* quantity, e.g. the number of molecules in a volume element Ω around x. This discrete character of the dynamical variables leads to internal fluctuations in the system. Only in a certain limit of large particle numbers one may expect these fluctuations to vanish asymptotically and the deterministic description to be valid. Thus, on a more refined, mesoscopic level the reaction–diffusion process has to be regarded as a discrete stochastic process.

In order to formulate this stochastic process physical space, i. e. the interval $[0, L]$, is discretized into a sufficiently large number M of cells labelled by the integer index $\lambda = 1, \ldots, M$. Doing so, we define a mesoscopic length scale $\Omega = L/M$ which is chosen in such a way that the system can be considered to be homogeneous within distances of the order Ω. Next we introduce for each cell λ a positive integer N_λ which denotes the number of molecules in cell λ. These numbers are regarded as time dependent random numbers, i. e. the set $(N_1, \ldots, N_M)$ represents a multivariate stochastic process.

Assuming that $(N_1(t), \ldots, N_M(t))$ is a Markov process, its dynamics is completely specified by giving a master equation for the probability distribution

$P(N_1, \ldots, N_M, t)$. The master equation is written in the form

$$\frac{\partial}{\partial t} P = \mathbf{A} P \tag{10}$$

where $\mathbf{A}$ is a linear time evolution operator acting on functions of the stochastic variables $(N_1, \ldots, N_M)$. We shall use the term *function* (of the stochastic variables) for a map from the state space $\{(N_1, \ldots, N_M)\}$ into the real numbers and denote them by normal type capital letters. An *operator*, denoted by a bold-face letter, maps a function of the stochastic variables to a function of the stochastic variables.

The expectation value $\langle F \rangle$ of an arbitrary function $F(N_1, \ldots, N_M)$ is

$$\langle F(t) \rangle = \sum_{N_1=0}^{\infty} \cdots \sum_{N_M=0}^{\infty} F(N_1, \ldots, N_M) P(N_1, \ldots, N_M, t) \quad . \tag{11}$$

In particular, the expectation value

$$c(x_\lambda, t) := \frac{1}{\Omega} \langle N_\lambda(t) \rangle \tag{12}$$

represents the average concentration of molecules in cell λ. Within a certain continuum limit the time evolution equation for the concentration (12) derived from the master equation converges to the Fisher–Kolmogorov equation. This continuum limit implies large occupation numbers N_λ and large concentrations, and will be discussed below.

The construction of the time evolution operator $\mathbf{A}$ is straightforward. Following [7, 8, 12] the diffusive part is modelled as a collective random walk, represented by $\mathbf{A}_d$, and the reactive part as a chemical birth–and–death process, represented by $\mathbf{A}_r$:

$$\mathbf{A} = \mathbf{A}_d + \mathbf{A}_r \quad .$$

It is convenient to introduce the shift operators $\mathbf{E}_\lambda$ and $\mathbf{E}_\lambda^{-1}$ [8], which are defined by:

$$\begin{aligned} \mathbf{E}_\lambda F(\ldots, N_\lambda, \ldots) &:= F(\ldots, N_\lambda + 1, \ldots) \quad , \\ \mathbf{E}_\lambda^{-1} F(\ldots, N_\lambda, \ldots) &:= \begin{cases} F(\ldots, N_\lambda - 1, \ldots) & \text{if} \quad N_\lambda \geq 1 \\ 0 & \text{if} \quad N_\lambda = 0 \end{cases} . \end{aligned}$$

These operators describe the creation and annihilation of the particles.

The reaction operator involves annihilation and creation of particles within the cells:

$$\mathbf{A}_r = \sum_{\lambda=1}^{M} \left(\mathbf{E}_\lambda^{-1} - \mathbf{1} \right) N_\lambda + \frac{1}{\Omega} \left(\mathbf{E}_\lambda - \mathbf{1} \right) N_\lambda \left(N_\lambda - 1 \right) \quad . \tag{13}$$

The creative transitions within cell λ, that correspond to the reaction $Y + X \rightarrow 2X$, cf. eqn. (2), are represented by the operator $(\mathbf{E}_\lambda^{-1} - \mathbf{1}) N_\lambda$, and the destructive transitions, that correspond to $Y + X \leftarrow 2X$, by $\left(\mathbf{E}_\lambda - \mathbf{1} \right) N_\lambda \left(N_\lambda - 1 \right) / \Omega$.

Any possible transition can be written as a product of the two elementary operators $\mathbf{E}_\lambda$ and $\mathbf{E}_{\lambda'}^{-1}$. The jump of a particle to another cell is equivalent to the annihilation of a particle in one cell and creation in the other. Jumps to the left are consequently represented by a term $\mathbf{E}_{\lambda-1}^{-1}\mathbf{E}_\lambda - \mathbf{1}$, jumps to the right by $\mathbf{E}_{\lambda+1}^{-1}\mathbf{E}_\lambda - \mathbf{1}$. The diffusion operator $\mathbf{A}_d$ describes the collective random walk of the particles:

$$\mathbf{A}_d = \frac{\gamma}{\Omega^2}\sum_{\lambda=1}^{M}\left(\mathbf{E}_{\lambda-1}^{-1}\mathbf{E}_\lambda + \mathbf{E}_{\lambda+1}^{-1}\mathbf{E}_\lambda - \mathbf{2}\right)N_\lambda \quad . \tag{14}$$

The boundary conditions are such that particles which jump to the left of cell 1 or to the right of cell M are immediately replaced. In equation (14) this may formally be expressed by identifying cells 0 and 1 as well as cells M and $M+1$. Since $\langle N_\lambda\rangle$ varies little with λ along the cells near the boundaries $\lambda = 1$ and $\lambda = M$ for the type of solutions we investigate (see figures 1, 5), these boundary conditions are a good approximation of an infinite continuation of physical space with boundary conditions of type (6).

In the remainder of this section we will investigate the relation between the master equation and the Fisher–Kolmogorov equation, and in which limit the expectation values (12) obey the Fisher–Kolmogorov equation. The quantity $c(x_\lambda, t) = \langle N_\lambda(t)\rangle/\Omega$ is useful only if the probability distribution $P(N_1, \ldots, N_M, t)$ is unimodal. This seems, in fact, to be the case in all our numerical solutions of the master equation (see section 4).

In a first approach, using (12), (11) and the master equation (10) we derive an equation of motion for the first moments $\langle N_\lambda\rangle$:

$$\Omega\frac{\partial c(x_\lambda,t)}{\partial t} = \frac{\partial}{\partial t}\langle N_\lambda(t)\rangle = \langle N_\lambda \mathbf{A}\rangle \quad . \tag{15}$$

It simplifies the algebra considerably to use the following form for the time evolution equation for the expectation value:

$$\frac{\partial}{\partial t}\langle N_\lambda\rangle = \langle [N_\lambda, \mathbf{A}]\rangle \quad , \tag{16}$$

where [,] is the commutator. The proof is found in [13]. It uses the fact that $\mathbf{A}$ conserves the normalization. In order to evaluate $[N_\lambda, \mathbf{A}]$, one uses $[N_\mu, \mathbf{E}_\lambda] = -\delta_{\mu,\lambda}\mathbf{E}_\lambda$, $\left[N_\mu, \mathbf{E}_\lambda^{-1}\right] = \delta_{\mu,\lambda}\mathbf{E}_\lambda^{-1}$ and $[N_\mu, \mathbf{1}] = [N_\mu, N_\lambda] = 0$. Thus we arrive at:

$$\frac{\partial}{\partial t}\langle N_\lambda\rangle = \frac{\gamma}{\Omega^2}(\langle N_{\lambda+1}\rangle - 2\langle N_\lambda\rangle + \langle N_{\lambda-1}\rangle) \;+\; \langle N_\lambda\rangle \;-\; \frac{1}{\Omega}\,\langle N_\lambda^2 - N_\lambda\rangle \quad . \tag{17}$$

This is the time evolution equation for the first moments $\langle N_\lambda(t)\rangle$ and follows exactly from the master equation. Equations for higher moments are derived similarly. An essential feature is that the equation for the $k-$th moment contains the $(k+1)$–th moment on the right hand side and, thus, an infinite hierarchy

of moment equations is obtained. However, if one crudely makes a Poissonian approximation

$$\langle N_\lambda^2 - N_\lambda \rangle \approx \langle N_\lambda \rangle^2 \quad , \tag{18}$$

equation (17) becomes the discretized Fisher–Kolmogorov equation:

$$\frac{\partial}{\partial t} c(x_\lambda) = \frac{\gamma}{\Omega^2}(c(x_{\lambda+1}) - 2c(x_\lambda) + c(x_{\lambda-1})) + c(x_\lambda) - c(x_\lambda)^2 \quad . \tag{19}$$

Clearly, we can only compare solutions of the Fisher–Kolmogorov equation with solutions of the discretized equation when the difference quotient is a good enough approximation for the differential operator. On the other hand side, the qualitative behaviour of the solutions will be the same in both cases, i. e. the existence of travelling wave solutions and some sort of speed selection mechanism.

However, as will be demonstrated in section 4 large and significant deviations from the Poisson–like behaviour (18) occur in the frontal region. One thus cannot make the assumption (18) without distorting the dynamics in the frontal region. This distortion might be more or less grave, depending on the size of Ω and on the quantity of interest. We will come back to this question below.

The moment equations can be used to construct an equation for the time derivative of the expectation value of a function F which is a polynomial in the $N_1, \ldots, N_M$. In particular, consider the total particle number

$$N_{tot} := \sum_{\lambda=1}^{M} N_\lambda. \tag{20}$$

This definition is analogous to eqn. (7). Furthermore, in analogy to eqn. (8), we define

$$v_M := \frac{d}{dt}\langle N_{tot} \rangle. \tag{21}$$

Using the moment equation (17) and neglecting boundary terms, we get the equivalent form

$$v_M = \sum_{\lambda=1}^{M} \langle N_\lambda \rangle \; - \; \frac{1}{\Omega}\langle N_\lambda^2 - N_\lambda \rangle \quad . \tag{22}$$

The quantities N_{tot} and v_M play a central rôle in this paper. Note that eqn. (21) provides an exact definition of the wave front speed of the stochastic process under consideration, without invoking the concept of stationarity in a comoving frame. Remember eqn. (5), where this concept was used to define and describe travelling wave solutions of the Fisher–Kolmogorov equation. In section 4 we will show that v_M and, in a certain sense, the front form have stable stationary values, whereas the process itself does not become stationary in any comoving frame. This underlines the usefulness of eqn. (21).

Let us now discuss a more systematic procedure to establish a relation between the master equation and the Fisher–Kolmogorov equation than cutting off the

moment equations (17) through the approximation (18). To this end, we consider an expansion method introduced by van Kampen [8]. The expansion parameter has to be identified from the parameters of the equation under study. Basically, it is required to have the properties of a volume ("system-size-expansion"). In the last part of this section, we will sketch how to perform the expansion. It yields a stability criterion, which we will find to be violated. The effect of this instability will be discussed, and in particular we will find it to be the origin of the breakdown of the Poissonian approximation (18).

In order to understand better the meaning of the expansion we first want to take a closer look at the parameters γ and Ω. The number of particles per cell in the stable state is $\langle N_\lambda \rangle = \Omega$. Thus Ω is a measure for the quantization of the concentration, one particle corresponds to a "concentration quantum" $\delta c = 1/\Omega$. Adjacent cells in the system are coupled through diffusion. According to the master equation, the relative probability of a diffusive transition compared to the probability of a reactive transition lies between $2\gamma/\Omega^2$ and γ/Ω^2 (the first value for nearly empty cells, the second one for filled up cells, $N_\lambda = \Omega$). The quantity

$$\tilde{\gamma} := \frac{\gamma}{\Omega^2}$$

is therefore a measure for the strength of the diffusive coupling of the cells. More exactly: $\tilde{\gamma}$ is the ratio between the diffusive displacement frequency and the typical reaction rate. If $\tilde{\gamma}$ is large, the occupation numbers N_λ cannot vary much between adjacent cells, due to the balancing effect of the diffusion, and the front must extend over a large number of cells. (In fact, this number can then be roughly estimated as $12\sqrt{\tilde{\gamma}}$ from approximate analytic solutions of the Fisher–Kolmogorov equation [3]). Similarly, $\tilde{\gamma}$ small implies a steep front. According to this heuristic argument, $\tilde{\gamma}$ is a measure for the quantization of space relative to the width of the wave front, which is the only length scale of the Fisher–Kolmogorov equation (3). Expressing $\tilde{\gamma}$ and Ω in terms of the dimensional parameters D, A, B corresponding to the dimensional Fisher–Kolmogorov equation (1) and of the dimensional cell size δl we have

$$\Omega = \frac{A}{B}\delta l \qquad \text{and} \qquad \tilde{\gamma} = \frac{D}{A\delta l^2} \quad .$$

Each pair $(\tilde{\gamma}, \Omega)$ corresponds to a 2-dimensional surface in the 4-dimensional parameter space of the $D, A, B, \delta l$. The master equations belonging to points on the same 2–surface are equivalent.

Returning to van Kampen's expansion, we clearly identify Ω as the correct expansion parameter. Since we do not want to change the spatial resolution through the expansion, $\tilde{\gamma}$ has to be held constant. The limit

$$\Omega \to \infty \qquad \text{and} \qquad \tilde{\gamma} = \frac{\gamma}{\Omega^2} = \text{const.} \tag{23}$$

that we are going to perform can be expressed as follows in the dimensional parameters:

$$B \to 0 \qquad \text{and} \qquad D, A, \delta l = \text{const.}$$

Recall that in the dimensional Fisher–Kolmogorov equation (1) the concentration to the left of the front is A/B, which tends to infinity in this limit. Thus, the increase of the occupation numbers N_λ in the limit (23) means increasing concentration of the substance under consideration while leaving the spatial structure unchanged.

The essential assumption of the expansion is that it is possible to split the stochastic process N_λ into two parts: the first part is a macroscopic variable Ωc_λ and must be a stable solution of a yet to be defined deterministic equation. The second part $\Omega^{\frac{1}{2}}\,\eta_\lambda$ describes small stochastic deviations around the deterministic value,

$$N_\lambda \;=\; \Omega\, c_\lambda + \sqrt{\Omega}\,\eta_\lambda \quad .$$

This assumption means that the probability distribution $P(N_1, \ldots, N_M, t)$ is a single sharp peak with a width which is of order $\Omega^{\frac{1}{2}}$ smaller than the range in which its position varies.

The transformation of variables from $(N_1, \ldots, N_M)$ to $(\eta_1, \ldots, \eta_M)$ induces, from the master equation for $P(N_1, \ldots, N_M, t)$, a master equation for the joint probability distribution $\Pi(\eta_1, \ldots, \eta_M, t)$ of the transformed stochastic process $(\eta_1, \ldots, \eta_M)$. Collecting terms of the same order in Ω, the leading term of order $\sqrt{\Omega}$ diverges in the limit $\Omega \to \infty$, unless the macroscopic variables c_λ fulfill the discretized Fisher–Kolmogorov equation (19). The next–to–leading order terms of the master equation for Π constitute a linear Fokker–Planck equation:

$$\frac{\partial \Pi}{\partial t} = \sum_{\mu,\lambda} -L_{\mu\lambda}\frac{\partial}{\partial \eta_\mu}\left(\eta_\lambda \Pi\right) + \frac{1}{2} D_{\mu\lambda}\frac{\partial^2}{\partial \eta_\mu \partial \eta_\lambda}\Pi \quad ,$$

where

$$\begin{aligned} L_{\mu\lambda} &= \tilde{\gamma}\left(\delta_{\mu,\lambda-1} - 2\delta_{\mu,\lambda} + \delta_{\mu,\lambda+1}\right) + \delta_{\mu,\lambda}\left(1 - 2c_\mu\right) \quad , \\ D_{\mu\lambda} &= \delta_{\mu,\lambda}\left[\tilde{\gamma}\left(c_{\lambda-1} + 2c_\lambda + c_{\lambda+1}\right) + c_\lambda + c_\lambda^2\right] \\ &- \tilde{\gamma}\delta_{\mu,\lambda-1}\left(c_{\lambda-1} + c_\lambda\right) - \tilde{\gamma}\delta_{\mu,\lambda+1}\left(c_{\lambda+1} + c_\lambda\right) \quad . \end{aligned} \tag{24}$$

The second term of the Fokker– Planck equation describes a multivariate diffusion process for the stochastic variables η_λ with the diffusion matrix $\mathbf{D}$. Since the Fokker–Planck equation is linear, its general solution is a nonstationary multivariate Gaussian process and thus can be completely characterized by its mean values and variances. The drift matrix $\mathbf{L}$ governs the time evolution of the expectation values of the η_λ,

$$\frac{\partial}{\partial t}\langle \eta_\lambda \rangle = \sum_\mu L_{\lambda\mu}\langle \eta_\mu \rangle \quad ,$$

or in continuous notation

$$\frac{\partial}{\partial t}\langle\eta(x,t)\rangle = \mathbf{L}(t)(\langle\eta(x,t)\rangle) \quad , \tag{25}$$

where $\mathbf{L}$(t) is the linear, time dependent operator

$$\mathbf{L}(t) = \gamma\frac{\partial^2}{\partial x^2} + 1 - 2c(x,t) \quad .$$

Note that $\mathbf{L}$ is the same operator as obtained by performing a linear stability analysis of the Fisher–Kolmogorov equation. A necessary criterion for the validity of the Ω-expansion is that fluctuations are always damped, in order to keep the probability distribution $\Pi(\eta_1,\ldots,\eta_M,t)$ unimodal and narrow. Thus the macroscopic dynamics, which is described by the Fisher–Kolmogorov equation, is required to be at least asymptotically stable in the sense of Lyapunov [8]. A discussion of the stability of travelling wave solutions can for example be found in [3]. We quote the result that they are stable to finite support perturbations in the comoving frame of reference of the wave: transforming eqn. (25) to the comoving frame one obtains

$$\frac{\partial}{\partial t}g(z,t) = \mathbf{H}g(z,t) \quad , \tag{26}$$

where $g(x,t) = \langle\eta(x-vt,t)\rangle$, $z = x - vt$, and

$$\mathbf{H} = \gamma\frac{\partial^2}{\partial z^2} + v\frac{\partial}{\partial z} + 1 - 2\phi(z) \quad . \tag{27}$$

The operator $\mathbf{H}$ is time independent because ϕ is stationary in the comoving frame, compare eqn. (5). Consequently, the above stability condition amounts to the requirement that all eigenvalues of $\mathbf{H}$ must have negative real parts. In fact, restricting the underlying function space to pertubations with finite support one finds that all eigenvalues of $\mathbf{H}$ are real and negative. Thus, the macroscopic solution is asymptotically stable in the sense of Lyapunov against finite support perturbations.

However, as is seen by differentiating eqn. (4) with respect to z, the space derivative of the macroscopic solution ϕ represents an eigenvector of $\mathbf{H}$ with eigenvalue zero,

$$\mathbf{H}g_0 = 0 \ , \quad g_0 := \frac{\partial\phi}{\partial z} \quad . \tag{28}$$

This fact, of course, reflects the translational invariance of the Fisher–Kolmogorov equation. Although g_0 has not a finite support it is of relevance in our context. Namely, since $g_0(z) \to 0$ for $z \to \pm\infty$, g_0 can be approximated by finite support perturbations with arbitrary accuracy.

We have now discussed the stability of wave solutions regarding the continuous drift operators $\mathbf{L}$, respectively $\mathbf{H}$. On the level of the discrete master equation, we

do not expect the situation to change a lot, and we will find in fact the following conclusions justified from the simulations: Firstly, the stability condition which is necessary for the applicability of the Ω–expansion is fulfilled for those perturbations which change the shape of the front (e.g. steepen or flatten the front) and leave its position unchanged. Secondly, perturbations which correspond to a translation along the x–axis and which do not alter the front shape are not damped and, therefore, violate the necessary condition of asymptotic stability.

Since translative fluctuations are not damped, the Ω–expansion breaks down at this point. However, we will show that it is possible to at least approximately separate their influence from that of the others. Consider an ensemble of wave fronts starting each with the same shape at the same position (i. e. $P(N_1, \ldots, N_M, t_0)$ is a δ–distribution). If Ω is not too small, each of them will approximately behave like the corresponding solution of the Fisher–Kolmogorov equation. According to the above, the *shape* of each front is hardly distorted by the fluctuations. However, in addition to their deterministic propagation, they receive small random displacements through the translative fluctuations which stay constant rather than tending to zero. Therefore, the random front position represents a stochastic process of diffusion type [8]. Obviously, the total particle number N_{tot} introduced above in eqn. (20) is a sensitive measure of the front position. One therefore expects N_{tot} to be a diffusion–type process. In the next section the situation will be investigated by means of stochastic simulations of the full master equation.

4 Simulation

One advantage of the master equation formulation of reaction–diffusion processes is that the master equation literally translates into a compact and simple numerical simulation algorithm. Basically, the simulation algorithm generates an ensemble of realizations of the stochastic process $(N_1(t), \ldots, N_M(t))$. From this ensemble, all quantities of interest can be estimated. The well–known simulation algorithm [14, 15, 16] consists of three basic steps:

1. Let us assume that at time t the state of the system is given by $(N_1, \ldots, N_M)$. In the first step, the time $t + \tau$ of the next transition is determined. The total transition rate, as can be read off the master equation, is

$$W_{tot} = \sum_{\lambda=1}^{M} W_\lambda \quad ,$$

where

$$W_\lambda = \sum_{\lambda=1}^{M} \frac{2\gamma}{\Omega^2} N_\lambda \; + \; N_\lambda \; + \; \frac{1}{\Omega} N_\lambda \left(N_\lambda - 1\right) \quad . \tag{29}$$

The probability for any transition to occur within the infinitesimal timestep $d\tau$ is $W_{tot}d\tau$. Consequently, the waiting time τ, i.e. the time the system remains in the state $(N_1, \ldots, N_M)$ until the next transition occurs, is exponentially distributed. The random number τ is generated from the uniformly distributed random number r on the interval $[0, 1]$ via the formula

$$\tau = -\frac{1}{W_{tot}} \ln r \quad .$$

2. In the second step, the actual transition that is to occur is chosen from all possible ones, and all variables are updated correspondingly. The set of all possible transitions decomposes naturally into groups labelled by λ. The group with label λ contains the reactive transitions that occur within cell λ and the diffusive transitions in which a particle jumps out of cell λ. As indicated in equation (29), W_λ is the transition rate for transitions of group λ. Now, a group λ is chosen with relative probability W_λ / W_{tot} with the help of the rejection method [16]. In our case, there are four transitions in each group:

   (a) Diffusive transitions:

$$\left.\begin{array}{l} N_\lambda \to N_\lambda - 1 \\ N_{\lambda-1} \to N_{\lambda-1} + 1 \end{array}\right\} \text{probability} = \frac{\gamma}{\Omega^2} N_\lambda / W_\lambda$$

$$\left.\begin{array}{l} N_\lambda \to N_\lambda - 1 \\ N_{\lambda+1} \to N_{\lambda+1} + 1 \end{array}\right\} \text{probability} = \frac{\gamma}{\Omega^2} N_\lambda / W_\lambda$$

   (b) Reactive transitions:

$$\begin{array}{ll} N_\lambda \to N_\lambda + 1 & \text{probability} = N_\lambda / W_\lambda \\ N_\lambda \to N_\lambda - 1 & \text{probability} = \dfrac{N_\lambda (N_\lambda - 1)}{\Omega \; W_\lambda} \end{array}$$

   Performing one of these transitions yields the state $(N_1(t+\tau), \ldots, N_M(t+\tau))$. The four probabilities add up to 1.

3. Repeat steps 1 and 2 until a desired final time is reached.

Finally, by generating a sufficiently large number of realizations of the stochastic process, one can evaluate the interesting quantities as ensemble averages.

As initial conditions we took a step profile

$$N_\lambda(t_0) = \begin{cases} \Omega \, , & \text{for} \quad \lambda \leq \lambda_0 \\ 0 \, , & \text{else} \end{cases}$$

and a smooth function that better approximates the final front from (compare eqn. (9)):

$$N_\lambda(t_0) = \text{round}\left(\frac{\Omega}{\{1+\exp\left[\alpha\left(\lambda-\lambda_0\right)\Omega\right]\}^2}\right) \quad , \tag{30}$$

where round(x) is the integer next to the real x. In an ensemble of realizations of the stochastic process, each starts with the same initial condition.

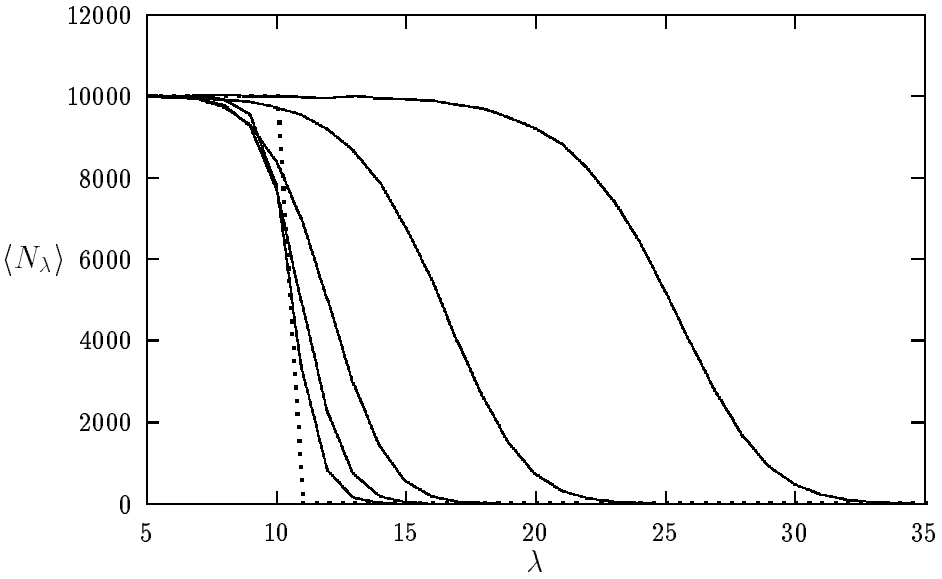

Figure 1:

The time development of the wave front for small times, starting from a step initial condition, obtained by averaging over 17 realizations. The parameters are $\Omega = 10^4$ and $\gamma = 10^8$, thus $\tilde{\gamma} = 1$. The dashed curve is the initial condition at time $t = 0$, the solid curves are the averages at times $t = 0.5, 1, 2, 5, 10$ (from left to right).

The time development of a wave front solution with $\Omega = 10^4$ and $\tilde{\gamma} = 1$ for small times, evolving from a step initial profile, can be seen in Fig. 1. The plotted front profiles result from averaging the occupation numbers of 17 realizations at equal times.

The most striking observed fact in our simulations is that the wave front speed v_M, calculated according to eqn. (21) or eqn. (22) relaxes to a stationary value different from $v_{min} = 2\sqrt{\gamma}$. Remember that v_{min} is the asymptotic speed of travelling wave solutions of the Fisher–Kolmogorov equation according to a theorem by Kolmogorov (see section 2). The relaxation of v_M is depicted in Fig. 2 for the step initial condition, $\Omega = 10^4$ and $\tilde{\gamma} = 1$, and in Fig. 3 for the smooth initial condition, $\Omega = 100$ and $\tilde{\gamma} = 10$. v_M according to (21) is

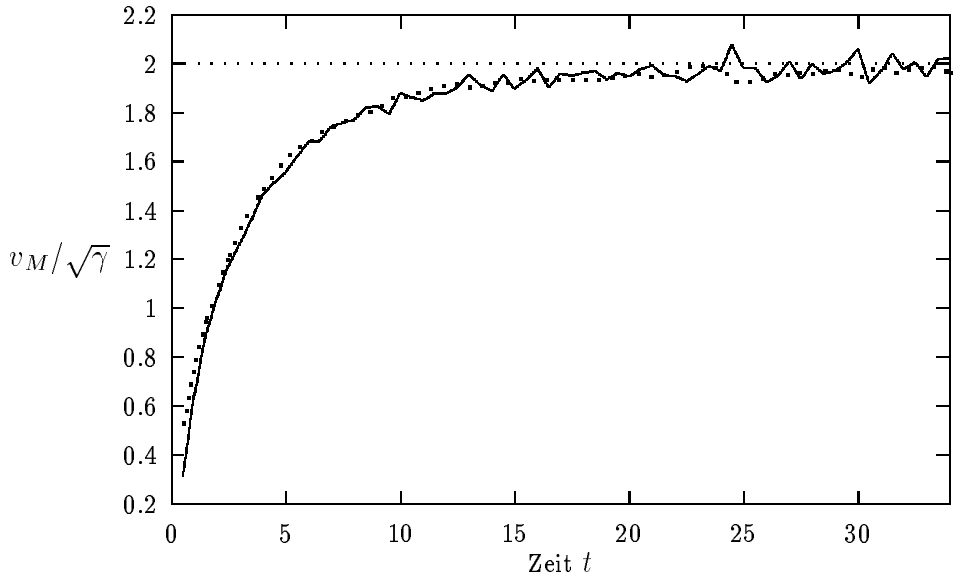

Figure 2:

The relaxation of the wave speed v_M. The data are taken from the same simulation as in Fig. 1, i.e. $\Omega = 10^4$, $\gamma = 10^8$, $\tilde{\gamma} = 1$ and a step initial condition. The solid line is $v_M/\sqrt{\gamma}$ calculated according to eqn. (21), the dashed line shows $v_M/\sqrt{\gamma}$ according to (22). The dotted line is at 2, which corresponds to the minimal wave speed $v_{min} = 2\sqrt{\gamma}$ belonging to the Fisher–Kolmogorov equation. The average value of the speed for $t \geq 20$ is $(1.985 \pm 0.004) \times \sqrt{\gamma}$ (compare Table 1).

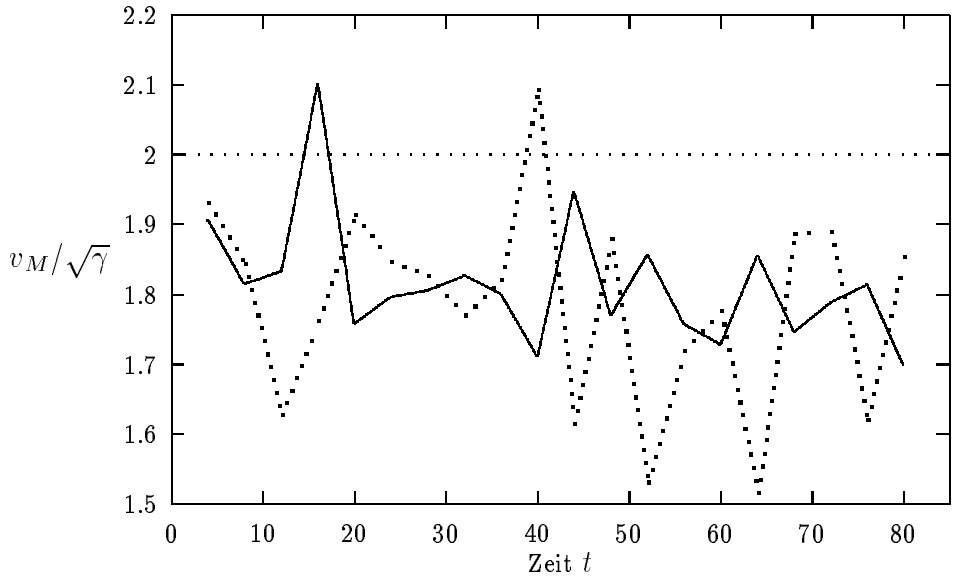

Figure 3:

The observed stationarity of the wave speed v_M for larger times. Here, $\Omega = 100$ and $\gamma = 10^5$, thus $\tilde{\gamma} = 10$. The initial condition was (30). As in Fig. 2, the solid line is $v_M/\sqrt{\gamma}$ calculated according to eqn. (21), the dashed line shows $v_M/\sqrt{\gamma}$ according to (22) and the dotted line at 2 corresponds to the minimal wave speed $v_{min} = 2\sqrt{\gamma}$. The average value of the speed for $t \geq 40$ is $(1.837 \pm 0.004) \times \sqrt{\gamma}$ (compare Table 1).

estimated by calculating the increase in the total number of particles within a certain time interval, averaged over a number of simulated realizations of the stochastic process. On the other hand, $\langle N_\lambda \rangle$ and $\langle N_\lambda^2 \rangle$ are directly estimated from the simulated realizations of the stochastic process, which gives a value for v_M according to (22). The difference between both estimations of v_M lies within the statistical errorbars. The time that the special analytic solution (9) needs to travel along the distance of its own width is of order $T_{relax} = 10$. This is also the timescale in which the wave front speed v_M approaches its stationary value. After times much larger than T_{relax} the initial condition will be forgotten (as long as it allows the development of a wave front at all). This is analogous to the wave speed selection mechanism for the Fisher–Kolmogorov equation described in section 2. Note that v_M stationary means that $\langle N_{tot} \rangle$ increases linearly.

In Table 1 we give an overview of the observed wave front speeds, divided by $\sqrt{\gamma}$, for a range of values of the parameters Ω and $\tilde{\gamma}$. The speeds were calculated according to equation (21) from the average of the particle production rate, and the errorbars of the speeds were calculated as the standard error of the mean. The averaging was made over a sample of $n \times m$ points, where n is the number of realizations and m is the number of equidistant times at which the speeds were measured. In each realization the first measurement was taken approximately after 5 relaxation times, followed by typically 40 more measurements; the time intervals between consecutive measurements were of the order of one relaxation time in order to ensure that consecutive measurements can be regarded as statistically independent. At this point we remark that for a simulation with large Ω, i.e. large cell occupation numbers, one needs less realizations than for one with small Ω to get the same statistical errors. A graphical representation of the lines $\tilde{\gamma} = 10$, 1, and 0.1 in this table is given in Fig. 4.

As we can see from Fig. 4 the line $\tilde{\gamma} = 1$ nicely converges for increasing Ω to the value of the Kolmogorov velocity v_{min}. Note that Ω has been varied over 5 orders of magnitude and that in order to obtain a wave front speed which is consistent with the value predicted from the Fisher–Kolmogorov equation Ω must at least of the order of 10^4. However, this does not mean that fluctuation effects then become negligible, as far as other observables such as the variance of the wave speed are concerned.

Furthermore, we see from Fig. 4 that the lines corresponding to different values of $\tilde{\gamma}$ exhibit a quite different behaviour. Taking into account that the number of cells located in the frontal region of a single realization of the wave is approximately $12\sqrt{\tilde{\gamma}}$ we conclude that the way in which the stationary wave speed v_M asymptotically reaches v_{min} for large Ω depends sensitively upon the width of the wave front.

Fig. 5 shows the occupation numbers N_λ taken at the same time from different realizations of the stochastic process. We see from this figure that the curves from different realizations emerge from each other by a shift along the λ–axis. In this sense, the shape of the wave front is stable. For comparison, the dashed line

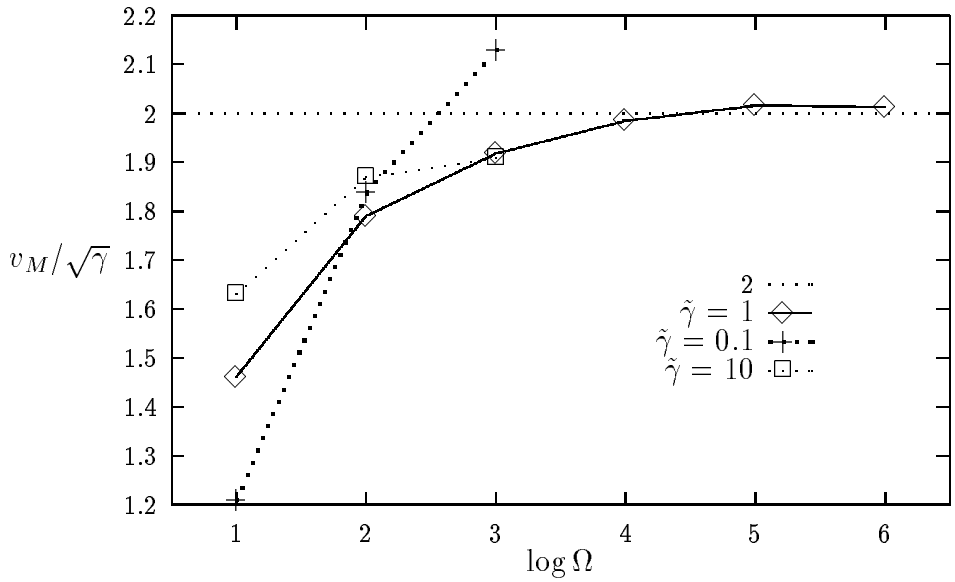

Figure 4:

The wave speed $v/\sqrt{\gamma}$ as function of Ω for $\tilde{\gamma} = 0.1, 1, 10$. v_M is estimated from simulation data according to eqn. (21).

indicates the shape of the special analytical solution (9), at an arbitrary position. In contrast, the expectation values $\langle N_\lambda \rangle$ describe a wave front shape which is much flatter, since they are the average over different realizations of the front which are at different positions. This observation confirms our discussion in section III: Each realization of the wave keeps its shape during its propagation while suffering random horizontal displacements. Whereas fluctuations which change the front shape are damped, translative fluctuations are unstable and give rise to a diffusive type behaviour of the random front position. In order to investigate this diffusion behaviour in more detail we plot in Fig. 6 the variance of the total particle number N_{tot},

$$\langle\langle N_{tot}^2 \rangle\rangle = \langle N_{tot}^2 \rangle - \langle N_{tot} \rangle^2 \quad . \tag{31}$$

As one can see $\langle\langle N_{tot}^2 \rangle\rangle$ increases linearly with time, which confirms the diffusive–type behaviour of the front position. From the figure we estimate the corresponding diffusion constant to be $\mathcal{D} \approx 8000$ for the given parameter values $\Omega = 100$, $\tilde{\gamma} = 10$.

The breakdown of the purely macroscopic description can also be seen by investigating the distribution of the N_λ. In Fig. 7 we have plotted the quantity

$$\Delta_\lambda := \langle N_\lambda^2 \rangle - \langle N_\lambda \rangle^2 - \langle N_\lambda \rangle \quad ,$$

which is a measure for the deviation from the Poissonian–type behaviour (cf. eqn. (18)), together with the mean front profile $\langle N_\lambda \rangle$ for 4 different times. As

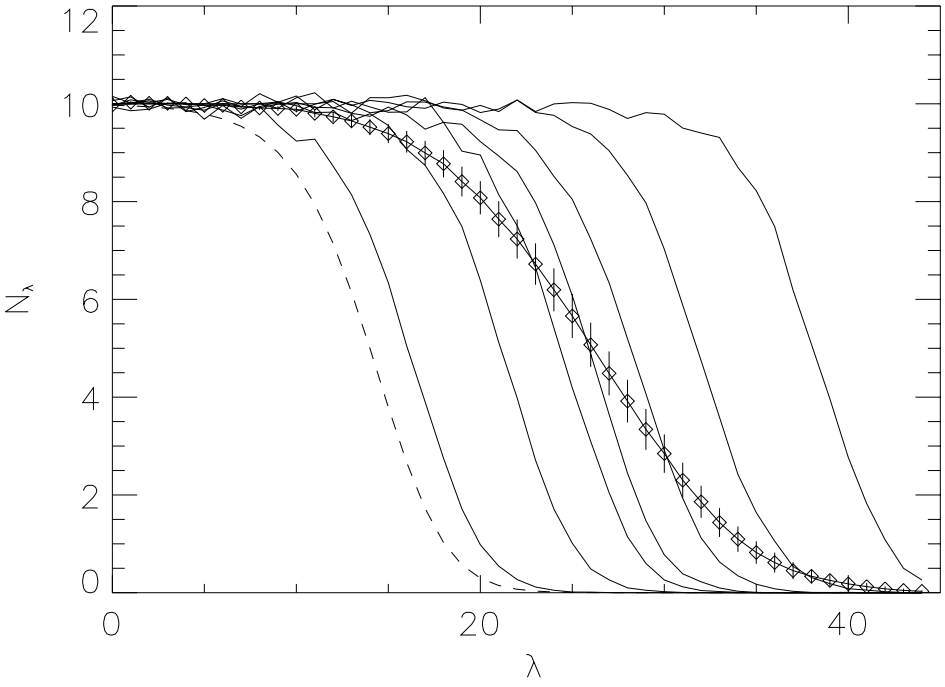

Figure 5:

The flattening of the averaged front profile due to the translative fluctuations. The 7 solid lines show 7 different realizations at the same time $t = 435$ for $\Omega = 10^4$, $\gamma = 10^8$ and $\tilde{\gamma} = 1$ (parameters as in Fig. 1 and 2). The symbols denote the average of 66 realizations, and the errorbars represent the standard error of the mean. For comparison, the dashed line indicates the special analytic solution (9) at an arbitrary position.

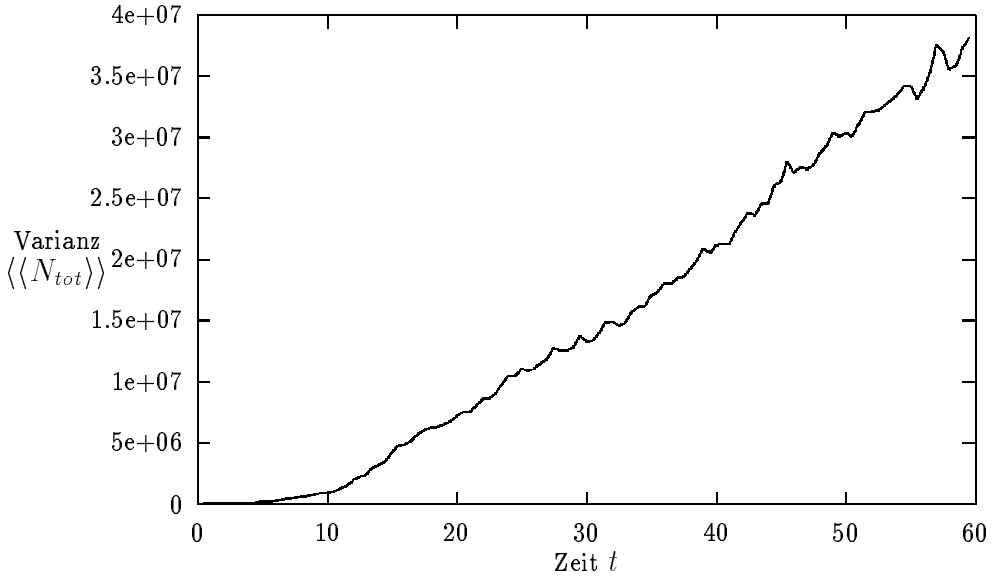

Figure 6:

The time development of the variance of the total particle number N_{tot}, see eqn. (20). The parameters are $\Omega = 100$, $\gamma = 10^5$, $\tilde{\gamma} = 10$, same as in Fig. 3.

is to be expected, Δ_λ is largest in the middle of the front, where the chemical reaction is fastest and the front is steepest, and vanishes outside the frontal region; it is approximately proportional to the derivative of the mean wave shape $\langle N_\lambda \rangle$. As in Fig. 6 we see that with increasing time the front broadens and that the deviation from the Poissonian becomes larger. One finds that $\sum_\lambda \Delta_\lambda$ grows proportional to the variance $\langle\langle N_{tot}^2 \rangle\rangle$.

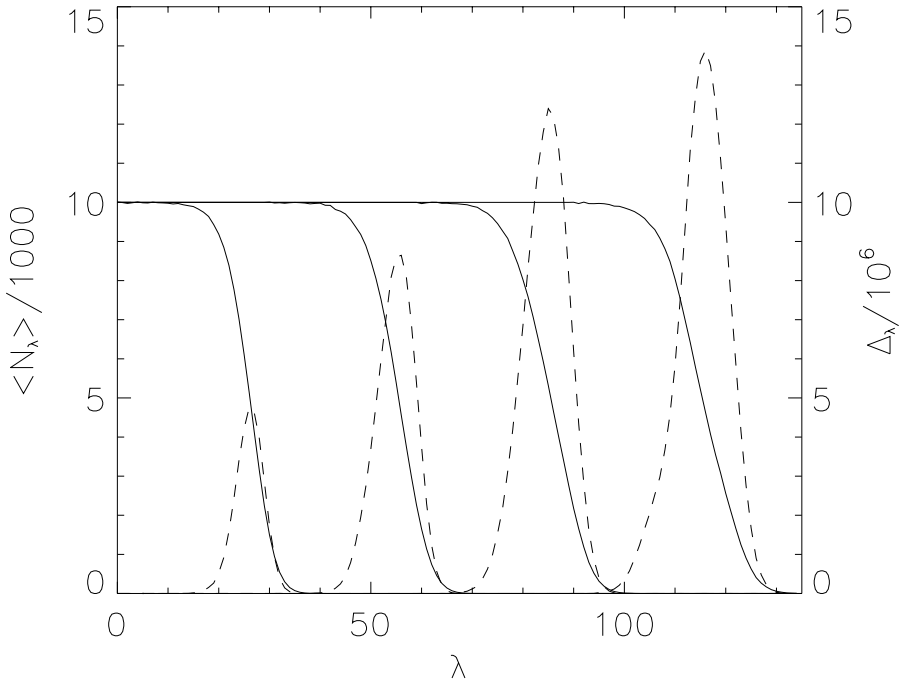

Figure 7:

The quantity Δ_λ (dashed lines), which measures the deviation of N_λ from the Poisson distribution, plotted together with the corresponding front profile $\langle N_\lambda \rangle$ (solid lines) at the four different times $t = 60, 135, 210, 285$. The parameters are $\Omega = 10^4$, $\gamma = 10^8$, $\tilde{\gamma} = 1$, same as in Fig. 1,2, and 5. The wave actually propagates about 149 cells in the time intervals $\Delta t = 75$ that lie between these four plots. Thus, in order to bring them together in one figure, the curves $\langle N_\lambda(t_i) \rangle$ and $\Delta_\lambda(t_i)$ are suitably shifted along the λ–axis.

Given a certain model, the informations presented in Fig. 4 can be used to estimate the influence of fluctuations on the wave front speed and to decide whether or not a continuous description in terms of the Fisher–Kolmogorov equation is

sufficient. As an example, we would like to relate the parameters $\tilde{\gamma}$ and Ω to an application of the Fisher–Kolmogorov equation which has already been given by Fisher [1]. Fisher used equation (1) to model the spread of an advantageous mutation in a population which is distributed uniformly in a linear habitat, such as a shoreline. He gives a numerical example with

$$D = \frac{L^2}{2\tau}, \qquad A = 0.01 \times \tau^{-1} \quad .$$

τ is the lifetime of one generation of the species, the standard displacement L of young from parents in each generation is assumed to be $L = 100$ yards and the selective advantage of the mutation A is 1 percent per generation. This information is sufficient to determine the minimum speed of wave front solutions, $v_{min} = 2\sqrt{AD} = 14$ yards per generation. We have to make additional assumptions on the cell size δl and on B in order to identify the corresponding master equation. Assuming $\delta l = q \times L$, where q is a small positive number, we get $\tilde{\gamma} = D/(A\delta l^2) = 1/(2q^2 A\tau) = 50/q^2$. A reasonable value for Ω, the number of individuals living on a length of $q \times 100$ yards may be in the order of 100. Locating Fisher's model in Fig. 4, it lies somewhere between the lines $\tilde{\gamma} = 10$ and $\tilde{\gamma} = 1$ around $\log \Omega \approx 2$. The fluctuation effect on the wave front speed is around 10 percent in this region. Furthermore, according to Fig. 6, the variance of the wave front position grows with approximately 70 yards^2/generation. Note that the discrepancy of the wave front speed between the Fisher–Kolmogorov equation equation and the master equation leads to completely different long–time predictions of the front position.

5 Conclusion

Let us briefly summarize the results of this paper. We have investigated the multivariate master equation which describes the reaction–diffusion process of the Fisher–Kolmogorov equation on a mesoscopic level. Performing stochastic simulations of this master equation we have demonstrated that fluctuations affect the speed of travelling waves. The asymptotic value of the wave speed can be larger or even lower than the minimal and stable value predicted by Kolmogorov's theorem for the macroscopic equation, depending on the values of the parameters in the master equation. Furthermore we found that the stochastic process which is defined as the fluctuating position of the wave front always exhibits a diffusion–type behaviour and is non–stationary even when the wave speed is stationary. Investigating the first variational equation of the Fisher–Kolmogorov equation this fact has been traced back to the existence of translative pertubations of the travelling wave which do not decay with time. Thus, the macroscopic dynamics turns out to be unstable and the Ω–expansion is, stricly speaking, not valid in general.

However, as we have discussed, the failure of the Ω–expansion does not mean that any connection between the stochastic process and the macroscopic equation, i. e. the Fisher–Kolmogorov equation is lost. This is due to the fact that all finite support fluctuations which change the front shape and leave the front position unchanged decay with time and fulfill the stability condition. This fact can be clearly seen in our simulations: Single realizations of the multivariate stochastic process exhibit a front shape which is both stable and constant in time. It is only the front position which suffers large fluctuations that lead to a broadening of the averaged wave front shape. Thus, although strictly speaking the assumptions of the Ω–expansion are not fulfilled many features predicted from this expansion remain valid. The important conclusion to be drawn is that the validity of any prediction made on the basis of the system–size expansion crucially depends on the observable under consideration.

In this paper we have not given an explanation for the deviations of the wave front speeds of the stochastic process from the Kolmogorov velocity v_{min}. The results of our stochastic simulations suggest that these deviations are caused by an asymmetrical influence of the large fluctuations of the wave front position upon its average drift. It should be clear that such an effect is neglected by the linear noise approximation of the Ω–expansion. However, a more detailed investigation of this effect can possibly be based on a modified Ω–expansion. Recall that the first variational equation admits stable and unstable solutions. Whereas the stable modes can be treated by the ordinary Ω–expansion method leading to the linear noise approximation, the unstable mode can be dealt with by the diffusion–type approximation in the sense of van Kampen [8] which yields a non–linear Fokker–Planck equation for the unstable mode. The general case can then be treated by decomposing the stochastic process into its stable and unstable part and performing the corresponding expansions separately. However, these more theoretical considerations are beyond the scope of the present paper.

Concluding, we remark that the described fluctuation effects on wave front propagation are not restricted to the special case of the Fisher–Kolmogorov equation , but can be expected to occur in more general reaction–diffusion systems which are translation invariant and which admit travelling wave solutions.

References

[1] R. A. Fisher, Annals of Eugenics **VII** (1936-37) 355-369.

[2] M. H. Cohen in Nonlinearity with Disorder, Springer Proc. in Physics, Vol.67, F. Abdullaev, A. R. Bishop, S. Pnevmatikos (Eds.) (Springer, Berlin Heidelberg, 1992) 161-170.

[3] J. D. Murray, Mathematical Biology, Biomathematics, Vol.19, (Springer, Berlin Heidelberg, 1989).

[4] M. S. Benilov, Physics Letters **A 169** (1992) 57-61.

[5] A. Lemarchand, H. Lemarchand, E. Sulpice and M. Mareschal, Physica **A 188** (1992) 277-283

[6] A. R. Kerstein, J. Stat. Phys. **45** (1986) 921-931.

[7] G. Nicolis, I. Prigogine, Self–Organization in Nonequilibrium Systems (A Wiley–Interscience publication, 1977).

[8] N. G. van Kampen, Stochastic Processes in Physics and Chemistry (Elsevier Science Publishers B.V., Amsterdam, 1992).

[9] M. Malek Mansour, C. van den Broeck, G. Nicolis, J. W. Turner, Ann. Phys. N. Y. **131** 283 (1981).

[10] A. Kolmogorov, I. Petrovsky, N. Piscounov, Bjulleten' Moskovskogo Gosudarstvennogo Universiteta, Sekcija A Matematika i mechanika. **1** (1937) 1-26.

[11] W. van Saarloos, Physical Review **A 37** (1988) 211-229.

[12] C. W. Gardiner, Handbook of Stochastic Methods, Springer series in synergetics, Vol. 13 (Springer, Berlin Heidelberg, 1985).

[13] H. P. Breuer and F. Petruccione, Physical Review **E 47** (1993) 1803-1814.

[14] D. T. Gillespie, Markov Processes (Academic Press Inc., San Diego, 1992).

[15] H. P. Breuer, J. Honerkamp and F. Petruccione, Chemical Physics Letters **190** (1992) 199-201.

[16] J. Honerkamp, Stochastic Dynamical Systems (VCH, New York, 1993).

Overview over simulated wave front speeds $v/\sqrt{\gamma}$						
	$\log \Omega$					
$\log \tilde{\gamma}$	1	2	3	4	5	6
2	1.75±0.02 42					
1	1.63±0.02 1080	1.87±0.01 1950	1.908±0.004 936		1.932±0.002* 28$^+$	
0	1.46±0.03 1600	1.79±0.02 1000	1.918±0.005 2340	1.985±0.003 380	2.017±0.003 936	2.013±0.003 30$^+$
-1	1.21±0.02 1600	1.84±0.01 1300	2.13±0.01 391			
-2	0.79±0.02 1600	2.21±0.02 490	2.92±0.03 400			
-3		2.07±0.03 720	4.67±0.06 750			
-4		0.92±0.02 396	5.9±0.1 672			

* $\log \tilde{\gamma} = 0.70$ for this entry.
$^+$ only one realization was generated.

Table 1: The wave speed $v_M/\sqrt{\gamma}$, obtained by means of eqn. (21) from the stochastic simulation data, as function of the parameters $\tilde{\gamma}$ and Ω. The numbers in the first lines of the boxes denote the mean value and the standard error of the mean, and the number in the second line of each box is the number of measurement points, as described in the text.